

## Angular Momentum Transfer in Deep Inelastic Heavy Ion Collisions - II

V. CARNEIRO BARBOSA, P. CARRILHO SOARES

*Instituto de Física, Universidade Federal do Rio de Janeiro, Caixa Postal 68528, Rio de Janeiro, 21941, RJ, Brasil*

and

E. CORRÊA DE OLIVEIRA, L.C. GOMES

*Centro Brasileiro de Pesquisas Físicas, Rua Dr. Xavier Sigaud 150, Rio de Janeiro, 22290, RJ, Brasil*

Recebido em 08 de outubro de 1985

**Abstract** The Fokker-Planck equation which describes the angular momentum transfer in deep inelastic heavy ion collisions is solved by a stochastic simulation procedure. The fusion cross section calculation is discussed. The calculations show that the critical orbital angular momentum does not play such a special role as in the deterministic case. The results of all the angular momentum transfer and their fluctuations are calculated and compared with experimental results for the reactions  $^{86}\text{Kr} + ^{154}\text{Sm}$  at 610 MeV,  $^{165}\text{Ho} + ^{148}\text{Sm}$ , and  $^{165}\text{Ho} + ^{176}\text{Yb}$  at 1400 MeV.

### 1. INTRODUCTION

The use of the Fokker-Planck (F.P.) equation in deep inelastic heavy ion collision was first proposed by Nörenberg<sup>1</sup>. Since then, the usual procedure for solving this equation has been the expansion of the probabilistic distribution function in its moments up to the second order<sup>2</sup>. Such a procedure is inadequate near the critical angular momentum. This inadequacy can be easily justified by remembering that the critical angular momentum characterizes an instability region of the underlying deterministic system. This has been exhibited in numerical solutions of the F.P. equation as obtained by Brosa and Cassing<sup>3</sup> for the case of two-dimensional phase space.

In this paper the F.P. equation is solved by a different procedure. We made use of the fact that the results of this equation are the same as predicted by the deterministic system subject to Langevin forces of adequate strengths. In this way, the distribution function was obtained by calculating nearly 18,000 orbits and observing the distributions of the pertinent variables in the asymptotic region. The underlying deterministic system used to describe the reactions is the

same as of reference 4. The strengths of the Langevin forces are fixed by imposing the Einstein's relations for the brownian motion. The temperature is calculated by imposing that the dissipated energy heats the compound system treated in the free Fermi gas model approximation. The only parameters which are free to be adjusted to the experimental data are the friction coefficients. These have already been fixed in ref. 4. Thus the simulation of the F.P. equation is done without any further adjustments.

We obtained a reasonable agreement with the experimental data for the angular momentum transfer in the reactions  $^{86}\text{Kr}+^{154}\text{Sm}$  at 610 MeV<sup>5</sup>,  $^{165}\text{Ho}+^{148}\text{Sm}$ , and  $^{165}\text{Ho}+^{176}\text{Yb}$  at 1400 MeV<sup>6</sup>. It is worth mentioning that we did not observe a sharp transition between the deep inelastic and fusion mechanisms when observed as a function of the initial orbital angular momentum (L). As a matter of fact, in the  $^{86}\text{Kr}+^{154}\text{Sm}$  reaction at 610 MeV for which the critical angular momentum is 197 A, the deep inelastic process still compete with the fusion mechanism even for values of the initial orbital angular momentum as low as 40 A.

In section 2 we give a brief description of the relations needed for the derivation of the F.P. equation and the method used to fix the temperature. In section 3 we give a description of the actual model employed in the present work and we indicate how to proceed with the simulation. In section 4 we exhibit our results and a discussion is presented in section 5.

## 2. THE FOKKER-PLANCK EQUATION

We assume  $H(q,p)$  to be the hamiltonian which describes the collective modes of the system that couple to the inelastic channels of a heavy ion collision. The effect of this coupling is assumed to be described by a stochastic force whose mean value gives the friction force and the fluctuating part is taken as a Langevin force. We therefore may write the following equations of motion

$$\dot{q}^i = \frac{\partial H}{\partial p_i}$$

$$\dot{p}_i = - \frac{\partial H}{\partial q^i} - i_{ij} \frac{\partial H}{\partial p_j} + \xi_i(t)$$

where  $\Gamma_{ij}$  is the friction coefficient tensor and  $\ell_i(t)$  is the Langevin force. We further assume that  $\ell_i(t)$  is normally distributed with

$$\langle \ell_i(t) \rangle = 0$$

and

$$\langle \ell_i(t) \ell_j(t') \rangle = 2 K_{ij} \delta(t-t') .$$

Using these assumptions we derive the F.P. equation for  $f(q,p;t)$ , the probabilistic distribution function for the collective motion of the system<sup>7,8</sup>

$$\frac{\partial f}{\partial t} + [f, H] = \frac{\partial}{\partial p_i} \left[ \Gamma_{ij} \frac{\partial H}{\partial p_j} f + K_{ij} \frac{\partial f}{\partial p_j} \right] .$$

Imposing that the Boltzmann distribution,

$$f(H) = \text{cte.} \cdot e^{-\frac{H}{T}} ,$$

is the equilibrium solution for the above equation, we obtain the Einstein's relation

$$K_{ij} = T \Gamma_{ij}$$

with T playing the role of the temperature of the system. The temperature of the system is fixed by the relation

$$U(T) = \int_{-\infty}^t \Gamma_{ij} \frac{\partial H}{\partial p_i} \frac{\partial H}{\partial p_j} dt'$$

where

$$U(T) = \frac{A}{8} T^2$$

is the internal energy of the compound system treated as a free Fermi gas<sup>9</sup> and A its mass number.

### 3. THE SIMULATION

From now on we assume that  $H$  is given by

$$H = \frac{1}{2\mu} \left( p^2 + \frac{L^2}{r^2} \right) + \frac{J_1^2}{2I_1} + \frac{J_2^2}{2I_2} + V(r)$$

where  $V(r)$  is the same potential energy given in reference 4.

The friction coefficient tensor is calculated from a Rayleigh dissipation function  $F$  also defined in reference 4 and which we reproduce here:

$$F = \frac{1}{2} \beta \Gamma(r) \left[ \dot{r}^2 + \alpha_1 r^2 \left( \dot{\theta} - \frac{R_1}{R_1+R_2} \omega_1 - \frac{R_2}{R_1+R_2} \omega_2 \right)^2 + \alpha_2 \bar{c}^2 (\omega_1 - \omega_2)^2 \right].$$

As a direct consequence of the equations of motion the total angular momentum of the collective modes is conserved in the absence of Langevin forces. We will restrict these forces in order to preserve this conservation law. In this way the orbital angular momentum of the system can be obtained from the relation

$$L = L_0 - (J_1 + J_2)$$

where  $L_0$  is the initial angular momentum of the system.

To generate the Langevin forces we integrate the equations of motion by finite difference in steps of  $\Delta t = 0.5 \times 10^{-23}$  s. At every step the Langevin forces are substituted by random impulses obtained from a normal distribution with zero mean values and covariance matrix  $(\sigma_{ij})$  given by:

$$\sigma_{ij} = 2 K_{ij} \Delta t = 2T \Gamma_{ij} \Delta t.$$

The temperature  $T$  in the above equation is calculated along each trajectory using the equation:

$$U(T(t)) = Q^*(t) = -Q(t) + \frac{Q^2(t)}{Q_0}$$

where  $Q(t)$  is the energy lost along the orbit. The inclusion of the additional term  $Q^2(t)/Q_0$ , the energy loss through the vibrational mechanism, is justified in reference 4.

In the case under consideration, we observe that the radial Langevin force is not correlated to the other ones. Therefore we set:

$$\Delta p = \sigma_p \cdot U_0$$

with

$$\sigma_r^2 = \sigma_{rr} = 2T \beta \Gamma(r) \Delta t ,$$

where  $U_0$  is a random normal variable of zero mean value and unit variance. The impulses given to  $J_1$  and  $J_2$  can be obtained in a similar way if one takes care of the correlation between them. We have then<sup>10</sup>

$$\Delta J_1 = \sigma_1 \cdot U_1$$

$$\Delta J_2 = \sigma_2 \left[ \rho U_1 + \sqrt{1-\rho^2} U_2 \right]$$

with

$$\rho = \frac{\sigma_{12}}{\sigma_1 \cdot \sigma_2}$$

and

$$\sigma_1^2 = \sigma_{11} = \left[ \alpha_1 \left( \frac{R_1}{R_1+R_2} \right)^2 r^2 + \alpha_2 \bar{c}^2 \right] \cdot \sigma_r^2$$

$$\sigma_2^2 = \sigma_{22} = \left[ \alpha_1 \left( \frac{R_2}{R_1+R_2} \right)^2 r^2 + \alpha_2 \bar{c}^2 \right] \cdot \sigma_r^2$$

$$\sigma_{12} = \left[ \alpha_1 \frac{R_1 R_2}{(R_1+R_2)^2} r^2 - \alpha_2 \bar{c}^2 \right] \cdot \sigma_r^2$$

The random variables  $U_1$  and  $U_2$  have the same properties of  $U_0$ .

We have simulated an average of 50 orbits for every value of  $L$ , starting from  $L = 40 \text{ \AA}$  up to the grazing value for each reaction in unit steps of  $\text{\AA}$ . In this way we simulated  $\sim 1 \times 10^4$  orbits for the  $^{86}\text{Kr} + ^{154}\text{Sm}$  case,  $\sim 2 \times 10^4$  orbits for the  $^{165}\text{Ho} + ^{148}\text{Sm}$  case, and  $\sim 2.3 \times 10^4$  orbits for the  $^{165}\text{Ho} + ^{176}\text{Yb}$  reaction. For each orbit we stored the asymptotic values of  $L$ ,  $J_1$ ,  $J_2$ ,  $Q^*$  and  $\theta$ . We also kept the collision time for each orbit, defining it in such a way as to have zero value in the grazing orbit case.

These data were analyzed with the help of a statistical package in which the statistical weight ( $w$ ) for each orbit was obtained through the relation:

$$w(b) = \frac{2\pi b \Delta b}{n(L_0)}$$

where  $n(L_0)$  is the total number of orbits for the given  $L_0$ ,  $b$  the cor-

responding impact parameter and  $\Delta b$  the step of  $b$  corresponding to  $\Delta L_0 = \hbar$ .

#### 4. RESULTS

Fig. 1 exhibits the deep inelastic and fusion differential cross sections as a function of the initial angular momentum ( $L_0$ ) for the  $^{86}\text{Kr}+^{154}\text{Sm}$  reaction at  $E_{\text{Lab}} = 610$  MeV. We observe rather small values for the fusion cross sections over the whole  $L$  range. Above 220 R and up to 276  $\hbar$  (the grazing value of  $L$ ), the fusion cross section is practically zero. The critical value of  $L$ , ( $L_{\text{CR}}$ ) in this case is 197 R. One observes that the transition of the fusion cross section in the region of  $L_{\text{CR}}$  is not as abrupt as it could be expected from a deterministic calculation. Therefore, one cannot just take the critical value of the angular momentum to determine the fusion cross section. In our case we adopted a limiting time  $\tau_{\text{FUS}}$  for the deep inelastic mechanism to occur. In fig. 1  $\tau_{\text{FUS}}$  was taken to be equal to  $3.5 \times 10^{-21}$  s. This time was obtained through the following argument. In the reaction under consideration, the maximum temperature reached by the compound system is approximately 3 MeV. We estimate the single-particle widths

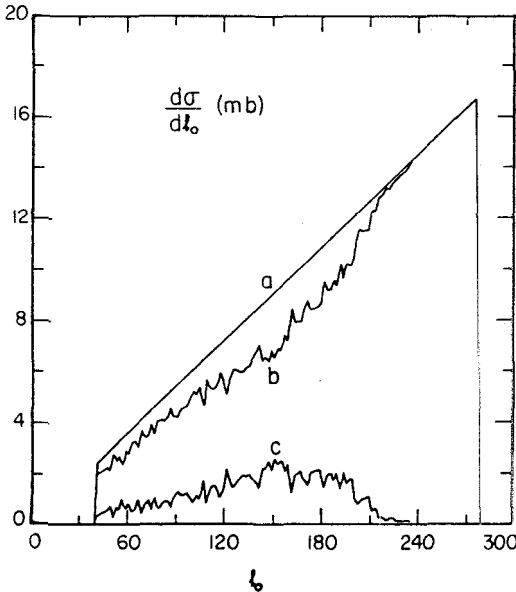


Fig.1 - The total (a), the deep inelastic (b) and the fusion (c) differential cross sections as a function of the initial angular momentum for the  $^{86}\text{Kr}+^{154}\text{Sm}$  reaction at 610 MeV. The horizontal scale is the initial angular momentum in units of  $\hbar$  ( $L_0 = l_0 \hbar$ ). The vertical scale is the  $d\sigma/dl_0$  in mb. The fusion cross section was obtained by assuming a maximum limiting time  $\tau_{\text{FUS}} = 3.5 \times 10^{-21}$  s and under the rolling assumption ( $\alpha_2 = 0$ ).

at this excitation energy to be close to 210 keV. The corresponding decay time is then approximately equal to  $3 \times 10^{-21}$  s. We take this time as a typical maximum time for the deep inelastic mechanism. The total fusion cross section ( $\sigma_{FUS}$ ) predicted by the corresponding deterministic system is 1180 mb. If we had taken  $\tau_{FUS} = 2.5 \times 10^{-21}$  s we would have obtained  $\sigma_{FUS} = 541$  mb. For  $\tau_{FUS} = 3.5 \times 10^{-21}$  s we obtained  $\sigma_{FUS} = 244$  mb. We observe that  $\sigma_{FUS}$  is rather sensitive to the value of  $\tau_{FUS}$ . One of the reasons for expecting such a sensitivity is that we make use of the proximity potential energy in our model. This potential energy gives a small binding for the di-nuclear system which is easily broken up by the thermal agitation. As a result, the longer the value of  $\tau_{FUS}$ , the smaller is  $\sigma_{FUS}$ .

Fig. 2 exhibits the mean value of the total angular momentum transferred to the ions ( $\langle J \rangle$ ) as a function of the  $Q^*$  for the reaction  $^{86}\text{Kr} + ^{154}\text{Sm}$  at 610 MeV of laboratory energy. The open dots were obtained from the experimental data<sup>5</sup> assuming  $\langle J_V \rangle = 14 \hbar$ . Curves b and c exhibit our results for two different values of  $\tau_{FUS}$  under the assumption of the rolling mechanism ( $\alpha_2 = 0$ ). One observes that  $\langle J \rangle$  is quite insensitive to the value of  $\tau_{FUS}$ . Curve a exhibits our results for the sticking mechanism ( $\alpha_2 = 0.5$ ) and  $\tau_{FUS} = 3.5 \times 10^{-21}$  s. We observe that the

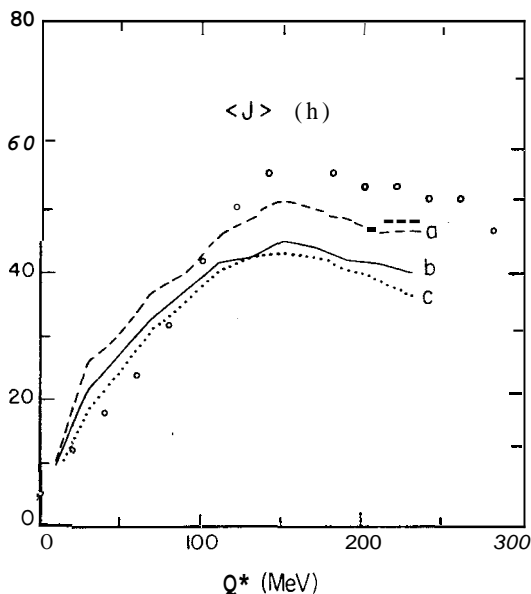


Fig.2 - The mean total angular momentum transfer  $\langle J \rangle$  in the  $^{86}\text{Kr} + ^{154}\text{Sm}$  reaction as a function of the energy loss ( $Q^*$ ). The horizontal scale is  $Q^*$  in units of MeV and the vertical scale is the mean total angular momentum transfer in units of  $\hbar$ . The open dots are the experimental data of reference 5 assuming  $\langle J_V \rangle = 14 \hbar$ . Curve a is the prediction of our model with the sticking assumption ( $\alpha_2 = 0.5$ ) and  $\tau_{FUS} = 3.5 \times 10^{-21}$  s. Curves b and c are the same as a but under the assumption of rolling mechanism. Curve b assumes  $\tau_{FUS} = 3.5 \times 10^{-21}$  s and curve c  $\tau_{FUS} = 2.5 \times 10^{-21}$  s.

stochastic simulation is somewhat sensitive to the sticking parameter and this hypothesis seems to give a better agreement with the experimental data. A similar effect was not found in the deterministic case. Another point worth mentioning is the fact that the simulated values of  $\langle J \rangle$  go up to  $Q^* = 250$  MeV while in the deterministic case, due to the fusion below  $L_{CR} = 197$   $\hbar$ , we could not obtain predictions of  $\langle J \rangle$  above  $Q^* = 150$  MeV.

Fig. 3 shows the standard deviation of the total angular momentum transfer ( $\sigma_J$ ) as a function of  $Q^*$  again in the reaction  $^{86}\text{Kr} + ^{154}\text{Sm}$  at 610 MeV. The open dots represent the experimental data<sup>5</sup> assuming  $\langle J_V \rangle = 14$   $\hbar$ . Curves b and c correspond to the simulated values for  $\tau_{FUS} = 3.5 \times 10^{-21}$  s and  $\tau_{FUS} = 2.5 \times 10^{-21}$  s, respectively, under the rolling assumption ( $\alpha_2=0$ ). Contrary to what happens with  $\langle J \rangle$ , the standard deviation  $\sigma_J$  is more sensitive to the value of  $\tau_{FUS}$ . Curve a corresponds to the sticking assumption ( $\alpha_2=0.5$ ), and  $\tau_{FUS} = 3.5 \times 10^{-21}$  s. It is worth mentioning that the sticking assumption contributes both to  $\langle J \rangle$  and to  $\sigma_J$  by increasing their values.

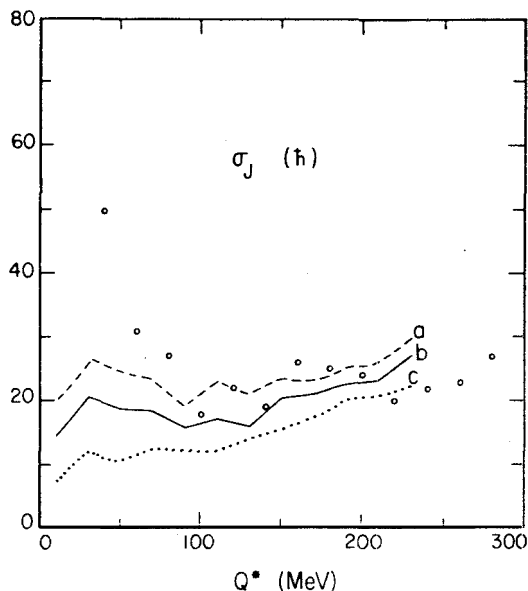


Fig.3 - The same as fig.2 but referring to the standard deviation of the angular momentum transfer in the  $^{86}\text{Kr} + ^{154}\text{Sm}$  reaction.

In figs. 4 and 5 we exhibit both the values of  $\langle J \rangle$  and of  $\sigma_J$  as a function of  $Q^*$  for the  $^{165}\text{Ho} + ^{148}\text{Sm}$  and  $^{165}\text{Ho} + ^{176}\text{Yb}$  reactions at



1400 MeV of laboratory energy. The open dots represent the experimental data<sup>6</sup> for  $\langle J \rangle$ . The simulated data (solid curves) reproduce essentially the deterministic results previously obtained<sup>4</sup>.

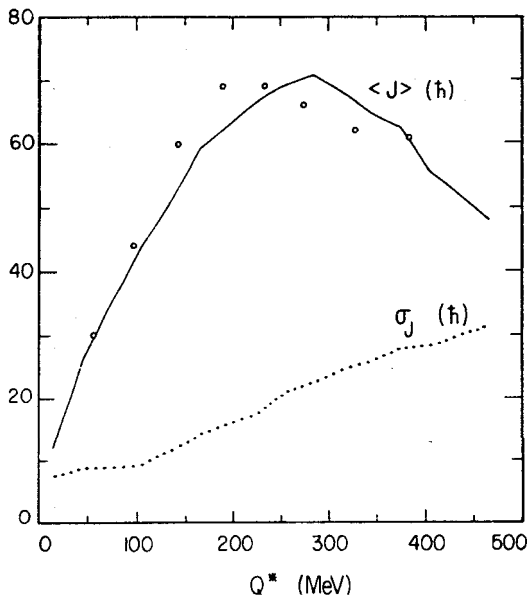


Fig.4 - The mean value  $\langle J \rangle$  and the standard deviation  $\sigma_J$  of the total angular momentum transfer as a function of  $Q^*$  for the  $^{165}\text{Ho} + ^{148}\text{Sm}$  reaction at 1400 MeV. The open dots are the experimental data for  $\langle J \rangle$  of reference 6. The two curves are our results for  $\langle J \rangle$  (solid curve) and  $\sigma_J$  (dotted curve). The horizontal and vertical scales are the same as in fig. 2.

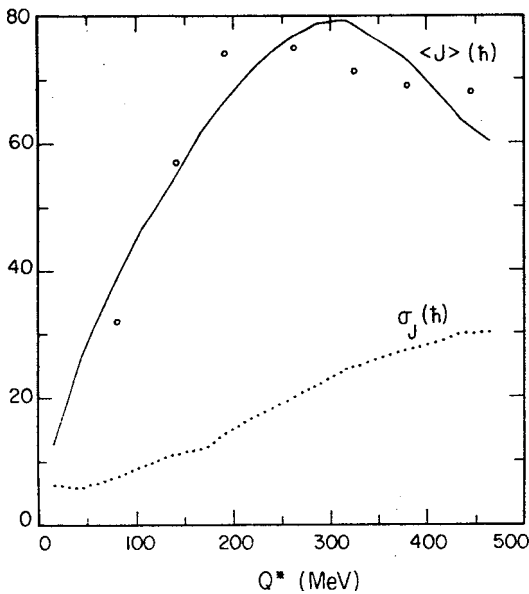


Fig.5 - The same as fig.4 but for the  $^{165}\text{Ho} + ^{176}\text{Yb}$  reaction at 1400 MeV.

The results exhibited in figs. 6, 7 and 8 for the case of the reaction  $^{16}\text{Ho} + ^{148}\text{Sm}$  at 1400 MeV allow us to discuss the use of  $Q^*$  as an experimental indicator of the value of  $L$ . Fig. 6 shows the mean value of  $L$ ,  $\langle L_0 \rangle$  for the simulated (solid curve) and deterministic (dotted curve) cases. The averages were taken over 30 MeV  $Q^*$  intervals in a way similar to the one utilized to analyze the experimental data. One observes that the two mean values do not differ in any substantial way. Fig. 7 shows the standard deviation of the initial angular momentum ( $\sigma_{L_0}$ ) as a function of  $Q^*$  also for both the simulated (solid curve) and the deterministic (dotted curve) cases. We observe here that although for the deterministic case the fluctuations lie around  $5 \hbar$  in the simulated case they have values of  $\sim 40 \hbar$ , i.e. close to ten times larger than in the deterministic case. This suggests that the use of the correlation between  $Q^*$  and  $L$ , predicted by the deterministic case should not be taken too seriously. This conclusion is reinforced by the result of the correlation coefficient ( $\rho(L_0, Q^*)$ ) exhibited in fig. 8. There one observes that for the simulated case the correlation coefficient is small (approximately -0.2) over most of the range of  $Q^*$ , while for the deterministic case this coefficient is obviously -1.

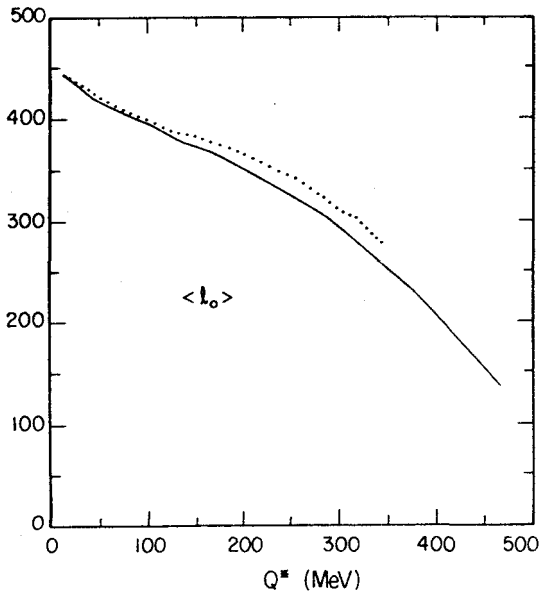


Fig.6 - The mean of the initial angular momentum as a function of  $Q^*$  for the  $^{16}\text{Ho} + ^{148}\text{Sm}$  reaction. The mean values were taken for every 30 MeV  $Q^*$  intervals. The solid curve refers to the simulated and the dotted one to the deterministic calculations. The horizontal and vertical scales are the same as in fig. 2

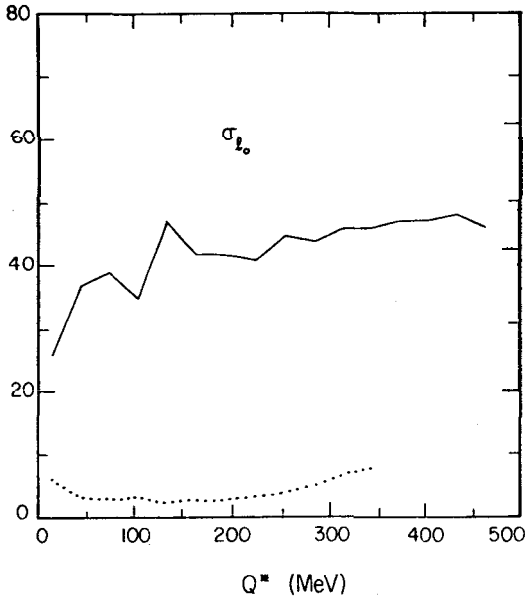


Fig.7 - The standard deviation of the initial angular momentum for 30 MeV  $Q^*$  intervals as a function of  $Q^*$  for the same reaction as of fig. 6. The horizontal and vertical scales are the same as in fig.2. The solid curve corresponds to the simulated and the dotted one to the deterministic calculations.

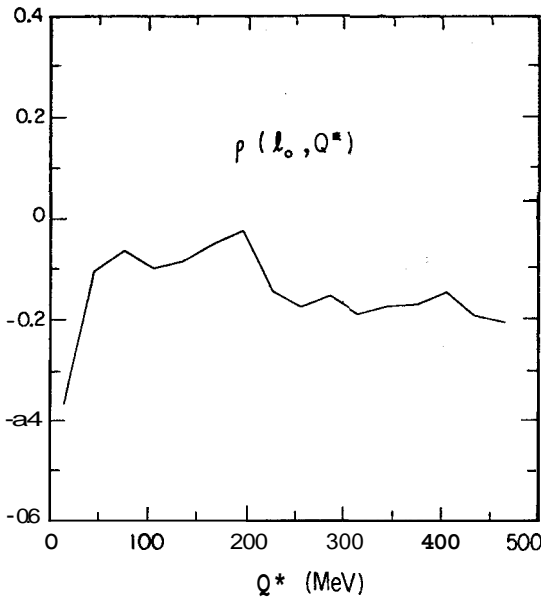


Fig.8 - The correlation coefficient of the  $L_0 Q^*$  pair of variables as a function of  $Q^*$  for the same reaction as of figs. 6 and 7. The horizontal scale is in units of MeV.

## 5. CONCLUSIONS

The existence of the critical orbits invalidates the use of expansion in moments of the probabilistic distribution functions near these critical regions of the phase space. The simulated approach is insensitive to such critical regions and its accuracy is dependent only on the amount of available computer time.

For the specific simulation presented here we were able to show that the fusion cross section is insensitive to the critical angular momentum but very sensitive to the maximum time allowed for the di-nuclear system to decay in deep inelastic channels. We believe that this lack of sensitivity has been greatly enhanced by the particular choice of the nuclear potential energy we made. If we had used a potential energy that gives a stronger binding energy to the di-nuclear system, the fusion cross section would have increased, approaching its deterministic value. The lack of experimental values for the fusion cross sections for the reactions studied did not allow us to further study this phenomenon. This result can be put in more general terms by saying that the simulated results are sensitive to the value of the transport coefficients over the extended region of the configuration space, contrarywise to what happens in the deterministic calculations which are sensitive only to the surface region.

It is worth mentioning that in the way the results were stored we could easily obtain plots of any single or double differential cross section and contour plots of the double differential cross sections.

The increase of computational facilities, mainly due to the advent of microcomputers, makes it possible to do simulations of stochastic processes, such as the one presented here, at low cost. In our opinion, simulations, such as this one, should be carried out in the future for the analysis of experimental data.

We would like to thank Profs. J. Lopes Neto and R. Donangelo for reading the manuscript.

## REFERENCES

1. W. Nörenberg, Phys. Lett. 52B, 289 (1974).
2. C. Ngô, H. Hofmann, Z. Phys. A282, 83 (1977); M. Berlinger, C. Ngô,

- P. Grangé, J. Richert, H. Hofmann, Z. Phys. A 284, 61 (1978); C. Riedel, G. Wolschin, Z. Phys. A294, 167 (1980).
3. U. Brosa, W. Cassing, Z. Phys. A294, 167 (1982).
  4. V.C. Barbosa, P. Carrilho Soares, E.C. Oliveira, L.C. Gomes, Rev. Bras. Fís. 14, 337 (1984).
  5. P.R. Christensen, Ole Hansen, O. Nathan, F. Videbaek, H. Freiesleben, H.C. Britt, S.Y. van der Werf, Nucl. Phys. A390, 336 (1982).
  6. A.J. Pacheco, G.J. Wozniak, R.J. McDonald, R.M. Diamond, C. C. Hsu, L.G. Moretto, D.J. Morrissey, L.G. Sobotka, F.S. Stephens, Nucl. Phys. A397, 313 (1983).
  7. R. Balescu, *Equilibrium and Nonequilibrium Statistical Mechanics*, John Wiley and Sons, New York (1975).
  8. J.R. Nix, Nuclear Dissipation in Heavy-Ion Reactions and Fission Preprint LA-UR-82-3651 (1982).
  9. Aa. Bohr, B.R. Mottelson, *Nuclear Structure*, Volume I, W.A. Benjamin, New York (1969).
  10. M. Abramowitz, I.A. Stegun (eds.), *Handbook of Mathematical Functions*, Dover Publications, New York (1970).

#### Resumo

A equação de Fokker-Planck para a transferência do momento angular nas reações muito inelásticas de íons pesados é resolvida por um método de simulação estocástica. A seção de choque de fusão é discutida e mostrada a descaracterização do momento angular orbital crítico das soluções determinísticas. Os resultados das transferências da momento angular e suas flutuações são obtidos e comparados com os resultados experimentais das reações  $^{86}\text{Kr} + ^{154}\text{Sm}$  a 610 MeV,  $^{165}\text{Ho} + ^{148}\text{Sm}$  e  $^{165}\text{Ho} + ^{176}\text{Yb}$  a 1400 MeV.